Enhanced Quasiparticle Heat Conduction in the Multigap Superconductor $Lu_2Fe_3Si_5$

Y. Machida,[1] S. Sakai,[1] K. Izawa,[1] H. Okuyama,[2] and T. Watanabe[2]

[1]*Department of Physics, Tokyo Institute of Technology, Meguro, Tokyo 152-8551, Japan*

[2]*Department of Physics, College of Science and Technology, Nihon University, Chiyoda, Tokyo 101-8308, Japan*

(Received 13 September 2010; published 11 March 2011)

Thermal transport measurements have been made on the Fe-based superconductor $Lu_2Fe_3Si_5$ ($T_c \sim 6$ K) down to a very low temperature $T_c/120$. The field and temperature dependences of the thermal conductivity confirm the multigap superconductivity with fully opened gaps on the whole Fermi surfaces. In comparison to MgB_2, $Lu_2Fe_3Si_5$ reveals a remarkably enhanced quasiparticle heat conduction in the mixed state. The results can be interpreted as a consequence of the unequal weight of the Fe 3d-electron character among the distinct bands.

DOI: 10.1103/PhysRevLett.106.107002 PACS numbers: 74.25.fc, 74.25.Jb, 74.25.Op, 74.70.Dd

Multigap superconductivity (MGSC) is the existence of gaps with significantly different magnitude on distinct Fermi surfaces (FSs). This phenomenon has been realized in a wide variety of materials [1–5], pointing to its universality underlying the superconductivity. One consequence of the MGSC is the ability to excite low-energy quasiparticles (QPs) due to the presence of the small gap, providing unusual features in the mixed state. Even though the MGSC has been extensively studied so far, the study has been mainly focused on the explanation for the anomalous properties. The recent discovery of the iron-pnictide superconductors [6], however, has offered further insight into the MGSC because electronic interactions and multiband structure are essential for the pairing mechanism [7]. In that sense, a question of how the electronic correlations affect on the MGSC is a fascinating issue to be addressed, which could not be examined on MgB_2. Unfortunately, the lack of high-quality samples and/or the high upper critical field prevent detailed studies of the MGSC in iron pnictides [7].

$Lu_2Fe_3Si_5$ is an another example of the Fe-based multigap superconductor with $T_c \sim 6$ K [8], which crystallizes in the tetragonal structure consisting of a quasi-one-dimensional iron chain along the c axis and quasi-two-dimensional iron squares parallel to the basal plane [9]. Band calculations predict that FSs consist of two holelike bands and one electronlike band, and each band has a contribution from the Fe 3d electrons [8]. In the holelike bands, some parts of the FSs have the different dimensionality reflecting the crystal structure [8]. Importantly, the Fe 3d electrons are responsible for the superconductivity, as suggested by the absence of superconductivity in the isoelectronic $Lu_2Ru_3Si_5$ and $Lu_2Os_3Si_5$ [10]. Therefore, $Lu_2Fe_3Si_5$ stands as the rare multigap superconductor with the d electrons in between the p-electron system (e.g., MgB_2 [1]) and the f-electron system such as $PrOs_4Sb_{12}$ [3], providing a unique opportunity to study the MGSC in the moderately correlated electron system.

The multigap superconductivity of $Lu_2Fe_3Si_5$ is first observed by the specific heat measurement down to 0.3 K under zero field [8]. It is of interest to further elucidate the MGSC by the thermal conductivity measurements down to lower temperature in the vortex state, because thermal conductivity is sensitive to the light carrier band which is expected to strongly affect low-energy QP excitations. The absence of the nuclear Schottky contribution is another advantage of this technique.

In this Letter, we report on the thermal transport measurements of single crystalline $Lu_2Fe_3Si_5$ down to $T_c/120$. Our detailed results of the thermal conductivity in the mixed state confirm the MGSC in $Lu_2Fe_3Si_5$. Moreover, from a comparative study with MgB_2, $Lu_2Fe_3Si_5$ reveals the significantly enhanced heat conduction as a consequence of the unequal weight of the Fe 3d-electron character among the distinct bands.

Single crystals were grown by the floating-zone method [11]. The sample was polished with a lapping paper down to a size of $1.40 \times 1.12 \times 0.28$ mm^3 to obtain the smooth surfaces. The one-heater-two-thermometer steady-state method was used to measure thermal conductivity. The heat current q was aligned along the [001] direction, and the magnetic field is applied parallel to the ab plane. The thermal contacts with a resistance of $\sim$10 mΩ were made by using a spot welding technique.

Figure 1 shows the temperature dependence of the thermal conductivity divided by temperature $\kappa(T)/T$ under zero field. An arrow denotes the superconducting transition temperature $T_c \sim 6$ K. As is clearly seen, $\kappa(T)/T$ shows a kink at T_c followed by a steep decrease with decreasing temperature. On further cooling, a hump structure appears around 3 K. The decrease of $\kappa(T)/T$ below T_c attributes to the reduction of the QP density by opening the gaps. On the other hand, the hump structure originates from an enhanced phonon mean-free path due to the condensation of electronic scattering centers. In fact, a similar enhancement of the phononic conductance (called phonon peak) is also observed in various materials such as Nb [12] and Pb [13]. The inset of Fig. 1 shows a κ/T vs T^2 plot. Since the measured κ contains both electron and phonon

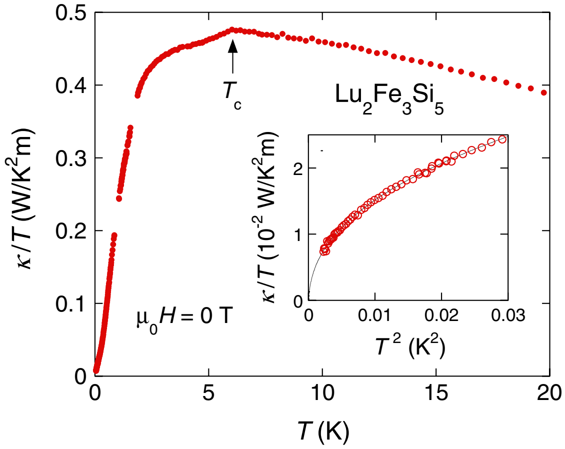

FIG. 1 (color online). Thermal conductivity κ/T as a function of the temperature under zero field. Inset: κ/T vs T^2 plot under zero field. The solid line represents a fit to the data by $\kappa/T = \kappa_0/T + bT^{\alpha-1}$.

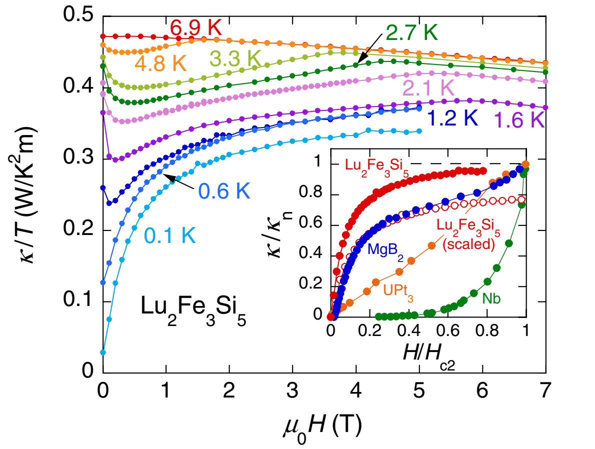

FIG. 2 (color online). Thermal conductivity κ/T as a function of the field at several temperatures. Inset: κ/κ_n vs H/H_{c2} plot at 0.1 K. For comparison, the data for Nb [17], MgB_2 [18], and UPt_3 [19] are also shown. The open circles show a result of scaling described in the text.

contributions, it is necessary to separate to each part as $\kappa = \kappa_e + \kappa_{ph}$. Below 0.15 K, κ/T is well described by a relation of $\kappa/T = \kappa_0/T + bT^{\alpha-1}$ with $\kappa_0/T = 0.000 \pm 0.005$ W/K^2 m, $b = 0.11$ W/K$^{2.8}$ m, and $\alpha \sim 1.8$. Here, we should note that the conventional T^3 dependence of κ_{ph} dominated by the ballistic phonon scattering fails to reproduce our result. The lower power of κ_{ph} with $\alpha \sim 1.8$ can be attributed to either the specular reflection of the phonon or the phonon scattering off the electrons [14–16]. The former is probable because of the smooth surfaces of our sample, while the latter seems to be unlikely in the superconducting state. The negligibly small κ_0/T in the zero temperature limit clearly indicates that $Lu_2Fe_3Si_5$ is a fully gapped superconductor consistent with the specific heat measurement [8].

Figure 2 shows the field dependence of $\kappa(H)/T$ at several temperatures. For $T \gtrsim 1.0$ K, $\kappa(H)/T$ takes a minimum at low fields and then increases with field. In general, the minimum of $\kappa(H)/T$ is explained as the result of the decrease of κ_{ph} due to the vortex scattering concomitant with the increase of κ_e resulting from the increase of the delocalized QP density [2,17,18]. Remarkably, for $T < 1.0$ K, $\kappa(H)/T$ shows a rapid increase and reaches almost half of the normal-state value κ_n/T already at low fields ($\mu_0 H < 1$ T). Here, κ_n/T is estimated from the Wiedemann-Franz law via $\kappa_n/T = L_0/\rho_0 = 0.325$ W/K^2 m, where $L_0 = 2.44 \times 10^{-8}$ W Ω/K^2 is the Lorenz number, and $\rho_0 = 7.5$ $\mu\Omega$ cm is the residual resistivity. It is of interest to compare our results with several superconductors. The inset of Fig. 2 depicts the normalized κ/κ_n at 0.1 K plotted against H/H_{c2} with the data for Nb [17], MgB_2 [18], and UPt_3 [19]. Here, the phonon thermal conductivity $\kappa(H = 0)$ is subtracted from κ/κ_n, and the upper critical field of $\mu_0 H_{c2} = 6.4$ T is obtained from Ref. [20]. The variation of κ/κ_n for $Lu_2Fe_3Si_5$ is in dramatic contrast with the behavior of the fully gapped s-wave superconductor Nb [17], in which small fields hardly affect κ/κ_n. By contrast, in nodal superconductor UPt_3, the delocalized QPs induced by the Doppler shift produces the remarkable increase of κ/κ_n. The strongly enhanced κ of $Lu_2Fe_3Si_5$ is a clear indication of either a nodal gap or nodeless multiple gaps. However, the nodal gap is ruled out by the absence of the κ_0/T term.

On the other hand, one immediately notices that $Lu_2Fe_3Si_5$ shares a striking resemblance with MgB_2, namely, a rapid increase of κ/κ_n at low fields and a saturation behavior at high fields, although κ/κ_n for $Lu_2Fe_3Si_5$ shows an even more pronounced increase and takes higher values. The field evolution of κ/κ_n of MgB_2 is well understood in terms of the multigap superconductivity with a small gap Δ_s on one FS and a large gap Δ_l on the other (indices l and s represent large and small gaps, respectively) [18]. A consequence of the small gap is an existence of a "virtual upper critical field" H_{c2}^s, above which the overlap of a huge vortex core provides a dramatic increase of the QPs contributed to the heat conduction. Here, we note that the anisotropic s-wave gap is denied in $Lu_2Fe_3Si_5$ as follows. If it is the case, the small gap Δ_s is regarded as a minimum value of the anisotropic gap Δ_{min}. So that, to induce the finite κ_e, a field of $H^* \sim 0.4$ T is required for the Doppler shift energy to overcome the minimum gap; $\Delta_{min} \ll \Delta_{max}(H^*/H_{c2})^{1/2}$ [21], where $\Delta_{max} \equiv \Delta_l$ [8]. Thus, in the anisotropic s-wave state, it is expected that κ/κ_n starts to grow above H^* due to the increase of Doppler shifted QPs. An absence of such behavior rules out the anisotropic s-wave gap.

The characteristic field scale of H_{c2}^s for the multigap can be estimated from $H_{c2}^s/H_{c2} \sim (\Delta_s/\Delta_l)^2(v_{F,l}/v_{F,s})^2$. On the other hand, the "normal-state" contribution of the small gap band κ_s/κ_n is obtained from $\kappa_s/\kappa_n = \kappa_s/(\kappa_l + \kappa_s) = N_s v_{F,s}^2 \tau_s/(N_l v_{F,l}^2 \tau_l + N_s v_{F,s}^2 \tau_s)$ via a relation of $\kappa_i \propto N_i v_{F,i}^2 \tau_i$, where N_i, $v_{F,i}$, and τ_i represent normal-state electronic densities of state, Fermi velocity, and the scattering rate of each gap band ($i = l, s$). Here, suppose τ_s/τ_l is close to unity, κ_s/κ_n is simplified to $\sim 1/\{1 + (N_l/N_s)(v_{F,l}/v_{F,s})^2\}$. Consequently, two-gap superconductivity is characterized by the three ratios Δ_l/Δ_s, N_l/N_s, and $v_{F,l}/v_{F,s}$. With the knowledge of $\Delta_l/\Delta_s \sim 4$ [1] and N_l/N_s, $v_{F,l}/v_{F,s} \sim 1$ [18], we find $H^s_{c2}/H_{c2} \sim 0.1$ and $\kappa_s/\kappa_n \sim 0.5$ for MgB_2 in agreement with various estimations [18,22]. Now, let us discuss the case of $Lu_2Fe_3Si_5$. Since $\Delta_l/\Delta_s \sim 4$ and $N_l/N_s \sim 1$ [8] the same as MgB_2, the κ/κ_n curve of $Lu_2Fe_3Si_5$ is expected to be scaled to that of MgB_2 by tuning the ratio of $v_{F,l}/v_{F,s}$. We achieve excellent scaling with $v_{F,l}/v_{F,s} \sim 0.8$ as shown by the open circles in the inset of Fig. 2, yielding $H^s_{c2}/H_{c2} \sim 0.04$ and $\kappa_s/\kappa_n \sim 0.6$. The deviation at high fields is due to the difference of H_{c2}. The inequality of $v_{F,l}/v_{F,s}$ indicates that the carrier mass m, which is inversely proportional to v_F, is different in each band for $Lu_2Fe_3Si_5$ in contrast to MgB_2 [18]. This contradiction might originate from the characteristic of the dominant electrons contributing to the density of state at the FS; Fe $3d$ electrons in $Lu_2Fe_3Si_5$ and B $2p$ electrons in MgB_2, respectively. In addition, unequal weight of the d character among the distinct FSs yields the heavy and light carrier bands. Notably, a signature of the electronic correlations possibly derived from the d electrons can be found in the specific heat coefficient $\gamma_n = 23.7$ mJ/mol K^2 [8], which is about 10 times larger than that of MgB_2 ($\gamma_n = 2.62$ mJ/mol K^2) [23]. The rather small $\gamma_{\text{band}} = 8.69$ mJ/mol K^2 obtained from the band calculations [8] also indicates the presence of the electronic interactions. On the other hand, the small gap on the light carrier band provides a dramatic enhancement of $\kappa(H)/T$ because κ is sensitive to the light carrier mass.

In order to further clarify the MGSC of $Lu_2Fe_3Si_5$, we present the $\kappa(T)/T$ curve in the vortex state (Fig. 3). By applying fields, we observe a pronounced increase of $\kappa(T)/T$ at low temperatures corresponding to the fast growth of $\kappa(H)/T$. Furthermore, an anomaly associated with a slight change of slope is found around 0.8 K at 0.1 T, and it shifts to ~0.3 K at 0.25 T as denoted by the arrows in Fig. 3. With further increasing fields, the anomaly becomes more pronounced, being a maximum around $T_m \sim 0.2$ K above 1.0 T. The maximum can be attributed to either the phononic or the electronic contribution. However, we exclude the phononic origin because the appearance of phonon peaks twice below T_c is highly unlikely. Moreover, an increase of the phonon mean-free path up to 10 folds of the zero-field value, for example, at 5 T, is improbable even if the low-temperature $\kappa(T)/T$ is dominated by the specular reflection. The effect of electron-phonon decoupling to the downturn of $\kappa(T)/T$ below T_m is also excluded because the $\kappa(H)/T$ curve at 0.1 K, which is well below T_m, shows even stronger field dependence compared with the data for $T = 0.6$ K $> T_m$ (Fig. 2). These results are in contradiction to the calculations in the presence of the electron-phonon decoupling [24], in which κ becomes insensitive to

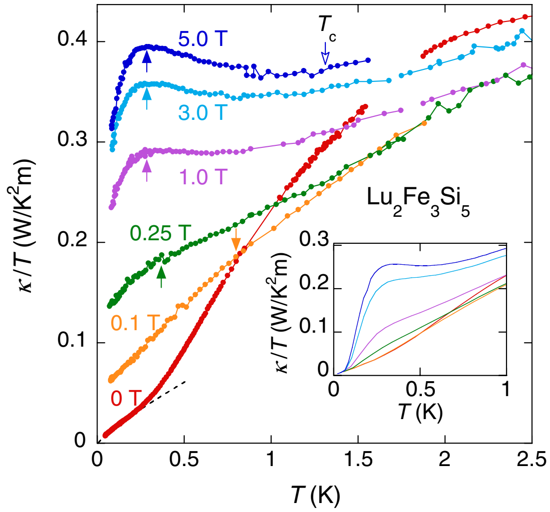

FIG. 3 (color online). Thermal conductivity κ/T as a function of the temperature under several magnetic fields. Inset: The calculated κ/T curves for the corresponding fields within the two-gap model described in the text.

the field as lowering the temperature due to the reduction of the electronic contribution. Thus, we turn to the electronic origin raising the following possibilities: (1) an enhancement of the QP mean-free path l_e, (2) a magnetic anomaly associated with a magnetic order, and (3) an increase of delocalized QPs excited above Δ_s. For the possibility of (1), the enhancement of l_e below T_c usually occurs as a result of the strong inelastic scattering. This is because normal-state l_e suppressed by the inelastic scattering starts to increase below T_c due to the condensation of electronic scattering centers. In practice, this behavior has been observed in $CeCoIn_5$ [25] and YBCO [26], in which a source of the inelastic scattering is attributed to the magnetic fluctuations. However, no signature of such fluctuation has been indicated in $Lu_2Fe_3Si_5$ [27]. The magnetic origin is also ruled out because Fe atoms carry no magnetic moment [27]. Therefore, in the following we discuss the possibility (3) by analyzing $\kappa(T)/T$ within the framework of the two-gap model.

In the superconducting state, κ_e is expressed as

$$\kappa_e/\kappa_n = \frac{2F_1(-y) + 2y\ln(1 + e^{-y}) + y^2(1 + e^y)^{-1}}{2F_1(0)}, \quad (1)$$

where $y = \Delta(t)/k_B T$, $\Delta(t)$ being half of the energy gap and $t = T/T_c$ [28]. $\Delta(t)$ is given by the standard gap interpolation formula $\Delta(t) = \Delta_0 \tanh(2.2\sqrt{1/t - 1})$, where Δ_0 is an energy gap at $T = 0$. The term of $F_1(-y)$ is given by $F_n(-y) = \int_0^\infty z^n(1 + e^{z+y})^{-1}dz$. Following the approach used for the specific heat [8], we generalize Eq. (1) to the two-gap model as $\kappa_e = n_s\kappa_{e,s} + (1 - n_s)\kappa_{e,l}$, where $\kappa_{e,i}$ ($i = l, s$) is the large and small gap bands' thermal conductivity, respectively, and n_s is a weight for the small gap band. In the analysis, n_s is fixed to be 0.6 regardless with the field, which is determined from the scaling. To obtain κ_n, we estimate κ_{ph} from the minima of $\kappa(H)/T$ (Fig. 2)

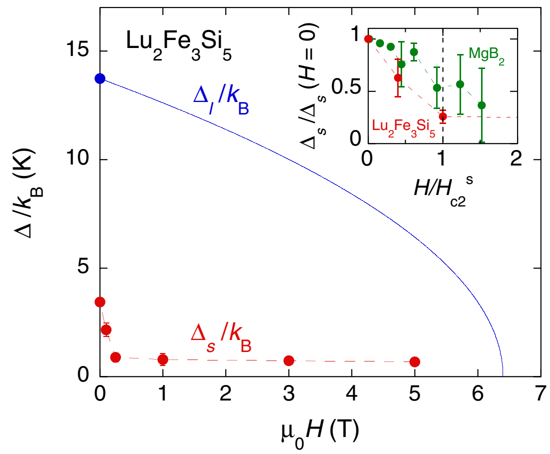

FIG. 4 (color online). Field dependence of the large and small superconducting gaps $\Delta_{l,s}/k_B$. The solid line denotes the calculated result of Δ_l/k_B based on the mean-field description. The dashed line is a guide to the eye. Inset: $\Delta_s/\Delta_s(H=0)$ vs H/H^s_{c2} plot for $Lu_2Fe_3Si_5$ and MgB_2 [30].

assuming that the minima represent at most the maximum value of κ_{ph} [18].

The solid lines shown in the inset of Fig. 3 represent the calculated results of the total thermal conductivity $\kappa/T = \kappa_e/T + \kappa_{\mathrm{ph}}/T$. Here, we assume $\kappa_{\mathrm{ph}}(T)/T$ to be $0.11T^{0.8}$ as determined by the zero-field κ/T (the dashed line in Fig. 3). Moreover, at zero field, we use the gap values of $2\Delta_{0,l}/k_BT_c = 4.4$ and $2\Delta_{0,s}/k_BT_c = 1.1$ obtained from the specific heat measurement [8]. The field variation of $\Delta_l(H)$ is assumed to follow the mean-field description $\Delta_l(H) = \Delta_{0,l}\sqrt{1 - H/H_{c2}}$ (the solid line in Fig. 4). It should be emphasized that the two-gap model well reproduces the experimental results especially for the maximum only by tuning the small gap Δ_s/k_BT_c. The result further supports the existence of the small gap in $Lu_2Fe_3Si_5$. Furthermore, the maximum most likely originates from an increase of the delocalized QPs excited over Δ_s. On the other hand, there exists a discrepancy between the experiment and the calculation below T_m; the experimental results show a gradual decrease while the calculated κ/T rapidly drops to zero. One possible interpretation is that the system behaves like a dirty superconductor ($\xi > l_e$) due to the presence of $\mu_0H^s_{c2}$ that gives rise to a large coherence length ξ. It has been argued that the superconductors in the dirty regime show a rapid growth of QP density in the mixed state in comparison with those in the clean limit ($\xi \ll l_e$) [29].

The parameter of Δ_s/k_B obtained from the analysis and Δ_l/k_B are plotted against the field in Fig. 4. It is clearly seen that Δ_s/k_B sharply decreases at low field $\mu_0H_s \leq$ 0.25 T, while Δ_l/k_B shows a monotonous decrease. Note that μ_0H_s is close to the virtual upper critical field $\mu_0H^s_{c2} \sim 0.26$ T. Interestingly, a similar suppression of Δ_s below $\mu_0H^s_{c2}$ is also observed in MgB_2 as demonstrated in the inset of Fig. 4, in which the gap values are determined by the point-contact study [30]. For MgB_2, this behavior is understood as a consequence of a weak interband pairing interaction [30,31]. From the analogy of MgB_2, the existence of the multiple bands having the different dimensionality and the weak interband interaction could be a source of the MGSC in $Lu_2Fe_3Si_5$.

In summary, our thermal conductivity measurements clarify the multigap superconductivity with the fully opened gaps in $Lu_2Fe_3Si_5$. The weak coupling between the distinct gap bands is thought to be the origin of the MGSC. In contrast to MgB_2, the dramatic enhancement of the quasiparticle heat conduction in the mixed state implies the presence of the electronic correlations derived from the Fe 3d electrons. Our findings shed new light on the MGSC in the correlated electron systems.

We thank H. Harima, H. Kusunose, Y. Nakajima, and Y. Yanase for discussions. This work is supported by Grants-in-Aid for Scientific Research from JSPS and for the Global COE Program from MEXT of Japan.

[1] F. Bouquet *et al.*, Europhys. Lett. **56**, 856 (2001).
[2] E. Boaknin *et al.*, Phys. Rev. Lett. **90**, 117003 (2003).
[3] G. Seyfarth *et al.*, Phys. Rev. Lett. **95**, 107004 (2005).
[4] Y. Kasahara *et al.*, Phys. Rev. Lett. **99**, 116402 (2007).
[5] G. Seyfarth *et al.*, Phys. Rev. Lett. **101**, 046401 (2008).
[6] Y. Kamihara *et al.*, J. Am. Chem. Soc. **130**, 3296 (2008).
[7] K. Ishida *et al.*, J. Phys. Soc. Jpn. **78**, 062001 (2009).
[8] Y. Nakajima *et al.*, Phys. Rev. Lett. **100**, 157001 (2008).
[9] H. F. Braun, *Ternary Superconductors* (North-Holland, Amsterdam, 1981), p. 225.
[10] D. C. Johnston and H. F. Braun, *Superconductivity Ternary Compounds II* (Springer-Verlag, Berlin, 1982).
[11] T. Watanabe *et al.*, Phys. Rev. B **80**, 100502(R) (2009).
[12] S. M. Wasim *et al.*, Phys. Rev. **187**, 539 (1969).
[13] M. H. Jericho, W. Odoni, and H. R. Ott, Phys. Rev. B **31**, 3124 (1985).
[14] W. S. Hurst *et al.*, Phys. Rev. **186**, 801 (1969).
[15] R. O. Pohl and B. Stritzker, Phys. Rev. B **25**, 3608 (1982).
[16] M. Sutherland *et al.*, Phys. Rev. B **67**, 174520 (2003).
[17] J. Lowell *et al.*, J. Low Temp. Phys. **3**, 65 (1970).
[18] A. V. Sologubenko *et al.*, Phys. Rev. B **66**, 014504 (2002).
[19] H. Suderow *et al.*, J. Low Temp. Phys. **108**, 11 (1997).
[20] Y. Nakajima *et al.*, Physica (Amsterdam) **469C**, 921 (2009).
[21] Y. Matsuda *et al.*, J. Phys. Condens. Matter **18**, R705 (2006).
[22] F. Bouquet *et al.*, Phys. Rev. Lett. **89**, 257001 (2002).
[23] H. J. Choi *et al.*, Nature (London) **418**, 758 (2002).
[24] M. F. Smith *et al.*, Phys. Rev. B **71**, 014506 (2005).
[25] Y. Kasahara *et al.*, Phys. Rev. B **72**, 214515 (2005).
[26] Y. Zhang *et al.*, Phys. Rev. Lett. **86**, 890 (2001).
[27] H. F. Braun *et al.*, J. Magn. Magn. Mater. **25**, 117 (1981).
[28] J. Bardeen *et al.*, Phys. Rev. **113**, 982 (1959).
[29] H. Kusunose, T. M. Rice, and M. Sigrist, Phys. Rev. B **66**, 214503 (2002).
[30] R. S. Gonnelli *et al.*, Phys. Rev. B **69**, 100504(R) (2004).
[31] A. E. Koshelev and A. A. Golubov, Phys. Rev. Lett. **90**, 177002 (2003).